arXiv:cond-mat/9611098v1 12 Nov 1996

Estimates of electronic interaction parameters for LaMO$_3$ compounds (M=Ti-Ni) from *ab-initio* approaches

Priya Mahadevan[1,2], N. Shanthi[1] and D. D. Sarma[1,*]

[1] *Solid State and Structural Chemistry Unit, Indian Institute of Science, Bangalore 560012, India*

[2] *Department of Physics, Indian Institute of Science, Bangalore 560012, India*

(February 1, 2008)

Abstract

We have analyzed the *ab-initio* local density approximation band structure calculations for the family of perovskite oxides, LaMO$_3$ with M=Ti-Ni within a parametrized nearest neighbor tight-binding model and extracted various interaction strengths. We study the systematics in these interaction parameters across the transition metal series and discuss the relevance of these in a many-body description of these oxides. The results obtained here compare well with estimates of these parameters obtained via analysis of electron spectroscopic results in conjunction with the Anderson impurity model. The dependence of the hopping interaction strength, t, is found to be approximately r^{-3}.

Introduction

Electronic structures of transition metal oxides have attracted a great deal of attention in recent years, arising from their unusual electronic and magnetic properties. Simultaneous presence of strong electron-electron interaction within the transition metal $3d$ manifold and a sizeable hopping interaction strength between the $3d$ and oxygen $2p$ states is primarily responsible for the wide range of properties exhibited by these compounds. Often the presence of a strong intraatomic coulomb interaction strength makes a single-particle description of such systems inadequate, necessitating a model many-body Hamiltonian approach [1,2]. However, such parametrized approaches require a prior knowledge of the various electronic interaction strengths, such as the intraatomic Coulomb interaction strength, U_{dd}, the charge-transfer energy, Δ, and the metal d-oxygen p hopping interaction strength, t, in order to provide a description of the ground state electronic structure. Traditionally, various high-energy spectroscopic results in conjuction with model Hamiltonian calculations have provided estimates for such interaction strengths [3–6]. However, it is well-known that wide ranges of parameter values are compatible with experimentally obtained spectra, leading to non-unique solutions [7]. This arises from the fact that the effect of a change in one parameter on the calculated spectrum can often be compensated by suitably changing another parameter, such that the the various solutions are indistinguishable within experimental uncertainties. This problem has given rise to different sets of estimates of interaction parameters from different groups for the same compound. In this context, it is highly desirable to obtain independent estimates of various interaction strengths from methods other than those using spectroscopic results. Even if only one interaction strength can be reliably estimated from any other method, the problem of non-uniqueness in analysing experimental spectroscopic result is considerably eliminated and such an approach will yield a more consistent description of the electronic structure.

Recently we have shown [8] that the electronic and magnetic structures of a particular class of transition metal oxides, namely the $3d$ transition metal perovskite oxides of the general formula LaMO$_3$ (M=Cr-Ni) are described very accurately within *ab-initio* approaches

based on local density approximation (LDA). Futhermore, it is also seen that the various excitation spectra, such as x-ray photoemission (XP) spectra of the valence band region and bremsstrahlung isochromat (BI) spectra of these compounds are also described well within the band structure approach. This success suggests that such band structure results could be useful in providing reliable estimates of various interaction strengths in this interesting class of compounds which have attracted a lot of attention in recent times [9]. Estimates of various interaction strengths based on *ab-initio* calculations have indeed been carried out in the past, for example for the $3d$ transition metal monoxide series [10], La_2NiO_4 [11], La_2CuO_4 [12], the $4d$ transition metal oxide, Sr_2RuO_4 [13] and Mn doped CdTe [14]. We report here the results of our analysis for the entire series of compounds belonging to the $LaMO_3$ family with M=Ti-Ni. Wherever possible, we compare the results obtained from the present approach with those obtained by analysis of various spectroscopic results already existent.

Methodology

We have performed detailed band structure calculations within the linearised muffin-tin orbital (LMTO) method using the atomic sphere approximation (ASA) [31]. Spin restricted calculations were performed for the real crystal structures experimentally observed. Thus, no attempt has been made to determine the lattice constants from total energy calculations. This is justified in the present context, since our primary aim here is to obtain strengths of the electronic interactions in the real systems with the observed lattice constants. In the case of $LaCoO_3$, however, we have performed calculations for various values of the lattice parameter in order to deduce the dependence of the hopping interaction strengths on distances. Analysis of these results shows that the present method predicts the lattice parameters with nearly 1% accuracy. $LaTiO_3$ [15], $LaVO_3$ [16], $LaCrO_3$ [17] and $LaFeO_3$ [18] in the observed Pbnm structure were calculated with twenty atoms in the unit cell, while $LaCoO_3$ [19] and $LaNiO_3$ [20] calculations were performed with ten atoms in the unit cell in the real $R\bar{3}c$ structure. In the case of $LaMnO_3$, the real crystal structure is Pnma stabilised by a Jahn-Teller distortion around the Mn-ions [21]. In contrast to all other

LaMO$_3$ compounds, this leads to a distorted octahedra of oxygens with two distinct Mn-O distances. Since, this would introduce additional parameters in the analysis, we have preferred to calculate the band structure of $LaMnO_3$ with an earlier reported R$\bar{3}$c idealised structure, where the Jahn-Teller distortion is suppressed [22]. Such approximations have been made in the past [23] and we do not expect to introduce any significant error in the parameters obtained, since the change in the interaction parameters is expected to be small for the small distortions observed.

Various interaction strengths can be estimated by mapping the band dispersions obtained from a parametrized tight-binding model onto those from *ab-initio* band calculations [10]. Since, we are primarily interested in the states arising from transition metal d-oxygen p interaction which dominate the occupied density of states as well as parts of the unoccupied states near the Fermi energy, E_F, the tight-binding Hamiltonian consists of the bare energies of the transition metal d (ϵ_d) and oxygen p (ϵ_p) states and hopping interactions between all these states. The nearest neighbor hopping interactions were expressed in terms of four Slater-Koster parameters, namely $pp\sigma$, $pp\pi$, $pd\sigma$ and $pd\pi$ [24]. It is further necessary [25] to include an interaction, $sd\sigma$, between the transition metal d and oxygen s states in order to simulate the splitting between the t_{2g} and e_g states at the Γ point, since the degeneracy of these two states is not lifted by the $p-d$ interaction at this symmetry point. In general, it is also necessary to include the effect of non-orthogonality of atomic functions located at different sites by considering the overlap matrix in such tight-binding approaches [25]. On the other hand, the tight-binding part of any parametrised many-body Hamiltonian, such as the Hubbard Hamiltonian, ignores the overlap matrix with an assumption of orthogonality of the basis functions. Since we are eventually interested in obtaining estimates of interaction strengths that enter such many-body Hamiltonians as parameters, we have carried out the fitting of the LMTO dispersions within two separate tight-binding models, one with and the other without the assumption of orthonormal basis functions.

Since we take into account only the transition metal d and oxygen p states, there are 56 bands to be fitted in the Pbnm structure and 28 bands in the R$\bar{3}$c structure. LMTO-ASA

results indicate that several of the low-lying bands within the nominal oxygen p-bandwidth have non-negligible contributions from La derived states. Thus, we have not taken into account some of these bands in the fitting procedure. We included the top 38 bands in the case of the Pbnm structure and 19 in the R$\bar{3}$c structure. In the case of $LaTiO_3$, the top 8 bands with mainly Ti d character overlap extensively with other bands having primarily La character. Thus we could not include these bands in the fitting procedure. We also checked the effect of including only the primarily transition metal d-derived bands, (top 20 in Pbnm and 10 in R$\bar{3}$c structures), leaving out all the primarily oxygen p-derived bands, from the fitting procedures. However, in the case of $LaTiO_3$ we have not carried out such an analysis due to the extensive overlap of Ti d and La derived bands mentioned above. Results of these different procedures, namely assuming the orthogonality or non-orthogonality of the atomic basis functions and employing different limited sets of bands, are consistent with each other.

Results and discussion

Total density of states as well as partial densities of Mn d and O p states in $LaMnO_3$ states obtained from LMTO-ASA calculations are shown in Fig. 1. We show the corresponding band dispersions along various symmetry directions in Fig. 2a. The zero of the energy scale corresponds to the Fermi energy, E_F. A set of two bands can be seen close to 3 eV at the Γ point and dispersing to higher energies along both $\Gamma - L$ and $\Gamma - Z$ directions, becoming larger than 4 eV halfway to the zone boundaries. These two bands are primarily La derived with negligible Mn d contributions (see Fig. 1) and we do not discuss these any further here. Next, one can observe a group of four strongly dispersing bands in Fig. 2a between about 0.5 and 3.5 eV giving rise to the approximately rectangular DOS marked A in Fig. 1. These bands are derived primarily from Mn $d(e_g)$-oxygen p-admixture with dominant Mn d character. Below the e_g bands, there is a group of 6 bands spread between -1 and 0.5 eV with considerably less dispersion than the e_g bands (Fig. 2a) giving rise to a narrow DOS marked B in Fig. 1. Various partial densities of states in this energy range suggest that this group has primarily Mn d character with some finite oxygen p admixture (Fig. 1). From these observations it is clear that this group of bands arises mainly from Mn d (t_{2g}) states.

Both e_g and t_{2g} bands discussed so far arise from Mn d-oxygen p antibonding combination, with dominant Mn d character. Thus, these bands are termed antibonding e_g^* and t_{2g}^* bands respectively. At still lower energies, we find an energy region with DOS between about -2.7 and -4.5 eV which is almost completely contributed by oxygen p-character with very small Mn d character. These features in the DOS are marked as C in Fig. 1 and arise from essentially oxygen-oxygen interactions with a non-bonding character with respect to Mn d- O p interactions. The corresponding dispersions of the eight bands can be observed in Fig. 2a. Dispersions of the remaining ten bands can be seen between -4 and -7.5 eV. The corresponding density of states (marked D) peaks at about -5.5 eV and has primarily oxygen p-character (see Fig. 1). However, finite Mn d admixture is also observable in this energy range. Thus, these states arise from oxygen p-Mn d bonding interactions and are the bonding counterparts of the Mn d-dominated antibonding e_g^* and t_{2g}^* bands at higher energies. These interpretations are consistent with the description of bonding in LaMO$_3$ compounds which have been discussed in detail in recent times [26–28].

In order to map the band dispersions obtained from LMTO-ASA calculations onto the tight-binding model, we have used all the ten primarily Mn d-derived e_g^* and t_{2g}^* bands as well as the top nine oxygen p-bands, as explained in the previous section. The best fit tight-binding dispersions are shown in Fig. 2b for comparison with the *ab-initio* calculated dispersions in Fig. 2a. It is evident from Fig. 2 that good agreement is obtained between the LMTO and tight-binding results; this is particularly true of the bands related to the t_{2g}^* and e_g^* distributed between -1 and 3.5 eV. This is significant, since the lower bands related primarily to oxygen p-states are completely filled in all these oxides and the electronic and magnetic properties in these cases are controlled entirely by the t_{2g}^* and e_g^* bands. Moreover, the present result suggests that the electronic structure of these transition metal oxides can be well described in terms of models involving only the transition metal d and oxygen p states (i.e $d-p$ models), as is the usual procedure.

While the above mentioned case of LaMnO$_3$ was calculated within the R$\bar{3}$c structure, we show an example of LMTO-ASA DOS and band dispersions for the Pbnm structure in

Figs. 3 and 4a respectively for $LaFeO_3$. Once again, four groups of DOS features are easily identified in Fig. 3 for $LaFeO_3$. These are marked A through D and have the same origin as discussed in the case of $LaMnO_3$ shown in Fig. 1. In the case of the Pbnm structure of $LaFeO_3$ however, there are twenty atoms in the unit cell, thereby doubling the number of bands in comparison with the previously discussed R$\bar{3}$c structure. Thus, within the $d-p$ part of the electronic structure alone, there are fifty-six bands; eight related to the e_g^* bands, twelve to the t_{2g}^* bands, sixteen related to the so-called non-bonding oxygen p-parts and twenty related to the bonding states of the Fe d-O p interactions. For the sake of clarity, we show the dispersions of those bands which are related to the e_g^* and t_{2g}^* bands with primarily Fe d character along various symmetry directions in Fig. 4a. The strongly dispersing group of eight bands (more easily recognisable along the $\Gamma - R$ direction) between about 0.5 eV and 3 eV arise from the e_g^* bands, while the considerably more flat twelve bands between -1 and 0.5 eV comprise the t_{2g}^* region. These band dispersions alongwith the sixteen non-bonding oxygen p bands were fitted with $d-p$ only tight-binding model along all symmetry directions in the same way as in the case of $LaMnO_3$. The resulting best fit tight-binding results are shown in Fig. 4b. Comparison of Figs. 4a and b indicate that the $d-p$ only nearest neighbor tight-binding model describes the band dispersions observed within the *ab-initio* calculation quite well.

The parameters for the best fits to the LMTO band dispersions for all the LaMO$_3$ compounds with M=Ti-Ni are given in Table I. While the main entries in this Table are for the cases where d and p bands were fitted, the numbers in parentheses are obtained by fitting only the e_g^* and t_{2g}^* bands. These two sets of estimates are very similar exhibiting some systematic changes across the transition metal series. We have plotted the strengths of various hopping interactions across the $3d$ transition metal series in Fig. 5. It is reasonable to expect that the variations in the hopping interactionwill be related to the changes in the relevant atomic distances. Thus, we have also shown the experimentally observed oxygen-oxygen (r_{O-O}) and the metal-oxygen (r_{M-O}) distances in the inset of Fig. 5. Both r_{O-O} and r_{M-O} appear to be larger in $LaFeO_3$ compared to the overall trend. This may arise from

the stability of the half-filled high-spin d^5 ionic configuration of Fe^{3+} in this compound. The decrease of these distances for $LaCoO_3$, just after $LaFeO_3$, is clearly related to the low-spin configuration of the Co^{3+} ion. Fig. 5 shows that the magnitude of $pp\sigma$ does not show any significant variations between V and Mn, then decreases for Fe followed by a substantial increase for Co. These variations in $pp\sigma$ strength can be easily related to the changes in the nearest neighbour oxygen-oxygen distances (r_{O-O}) in the LaMO$_3$ compounds; r_{O-O} substantially increases for $LaFeO_3$ giving rise to the observed decrease in $pp\sigma$ in this compound. For $LaCoO_3$, r_{O-O} is seen to be the smallest in the LaMO$_3$ series and for $LaTiO_3$, r_{O-O} is the largest; consequently the corresponding strengths of $pp\sigma$ are the largest and the smallest respectively in the series. Various transition metal d-oxygen orbital interactions, namely $sd\sigma$, $pd\sigma$ and $pd\pi$ also exhibit systematic variations across the series, the qualitative behaviour of these three interactions being quite similar to each other (Fig. 5). These interactions, besides being influenced by the transition metal-oxygen distance (r_{M-O}) shown in the inset, are also influenced by the spatial extent of the transition metal d orbitals. It is well-known that the d-orbitals contract across the transition metal series. Thus, the decreasing trends in the hopping interaction strengths between the transition metal d and oxygen orbitals between Ti and Mn, inspite of a small decrease in r_{M-O} arise from the d-orbital contraction across the series. Interestingly, the interaction strengths are larger for $LaCoO_3$ than $LaFeO_3$. This is clearly related to the pronounced decrease of r_{M-O} between $LaFeO_3$ and $LaCoO_3$, associated with the low-spin configuration in $LaCoO_3$ in contrast to the high-spin configuration in all the other LaMO$_3$ compounds with M=Ti-Fe.

Besides the various hopping interaction strengths, the bare energy difference, $(\epsilon_d - \epsilon_p)$, between the transition metal d and oxygen p orbitals exhibits a monotonic decrease across the LaMO$_3$ series, as shown in Fig. 6. This is indeed the expected trend, since the transition metal d level is increasingly stablized with respect to the oxygen p-orbital due to the increasing nuclear potential with increasing atomic number of the transition metal ion.

The results summarized in Table I and Figs. 5 and 6 are obtained by fitting the LMTO band dispersions to the results of the tight-binding model with finite overlap between the

orbitals at different atomic sites. However, most of the model many-body Hamiltonian approaches assume an orthogonal basis set; thus, the results in Table I cannot be directly used to estimate the parameter strengths appearing in such models. In order to provide estimates for such interaction strengths that parametrize the many-body calculations, we have also fitted the LMTO band dispersions with the results of a tight-binding Hamiltonian assuming an orthogonal basis. Thus, the tight-binding model corresponds to the one-electron part of the multiband Hubbard model involving all the transition metal d and oxygen p orbitals, suitable for the LaMO$_3$ series. The resulting estimates of the various interaction strengths corresponding to the best simulation of LMTO band dispersions are given in Table II. A comparison of Tables I and II show that the estimates of various parameters are quite similar in the two cases, justifying the assumption of an orthogonal basis in describing the electronic structures of these compounds. This is further supported by the fact that the orbital overlaps required to optimize the simulation of LMTO band dispersions are generally very small. We also find that the parameter values summarized in Table II exhibit similar systematic trends across the transition metal series as those in Table I (see Figs. 5 and 6).

In order to verify the relevance of the interaction parameters thus estimated, we note that there have been several attempts in the past to estimate many of these from various high-energy spectroscopic results in conjunction with different many-body approaches [29]. It is well known that such estimates are often non-unique [7]; however it is believed that in particular, various hopping interaction strengths can be estimated with a fair degree of accuracy from such approaches. Thus, we compare the estimates of the transition metal d-oxygen p interaction, $pd\sigma$ obtained from high-energy spectroscopy and the present approach. Two different groups have systematically worked on obtaining these experimental estimates for LaMO$_3$ compounds. In Fig. 7, we have plotted the experimentally obtained estimates of $pd\sigma$ from the Tokyo group [3] and the Bangalore group [5] against the estimates obtained in the present work. We show the results from these two groups using different symbols; we have drawn two broken lines as guides to the eye for the average overall variation of $pd\sigma$ across the series, as obtained by each of the two groups. The solid line in Fig. 7 with a unity

slope and no intercept, represents the behaviour of $pd\sigma$, if the experimental estimates and the present estimates were identical in every case. Obviously, the experimental estimates are somewhat different from the calculated ones. However, it is clear that the average variations of $pd\sigma$ across the series obtained by these groups are very similar to that suggested by the present calculations; this is indicated by the fact that the broken lines representing the average variation of experimentally obtained $pd\sigma$ are approximately parallel to the solid line within the accuracy of experimental estimates. Moreover, while the estimate of $pd\sigma$ from one group is higher than the calculated ones, the estimate from the other is consistently lower. This arises from the non-uniqueness of the parameter strengths estimated from experimental results discussed earlier. More importantly, it is obvious that $pd\sigma$ values estimated in the present work are also compatible with the high-energy spectroscopic data, since values both larger and smaller than the calculated values provide satisfactory description of the experimental observations. Thus, it is desirable to constrain the strength of $pd\sigma$ to the values calculated here on the basis of *ab-initio* approaches; this will avoid the problem of non-uniqueness normally encountered in such analysis [7] and will help in obtaining considerably better defined estimates of other parameters in the model.

The estimates of $\epsilon_d - \epsilon_p$ obtained by analysing the LMTO results can be related in an approximate way to the charge transfer energy, Δ defined [1] within the Anderson impurity Hamiltonian which is often used to provide a many-body description of the electronic structure of these oxides. For this, we first note that the eigen values, ϵ_d and ϵ_p in an LDA calculation are not directly related to the orbital ionization energies. In order to see the relationship between the charge transfer energy and the eigen values, we note that the total energy E within the LDA calculation can be expressed as a Taylor series expansion in terms of the electron occupancies, n_i, of the various levels i:

$$E(...n_i...) = E_0 + \sum_i b_i n_i + \sum_{ij} a_{ij} n_i n_j + ...$$

Retaining terms upto the second order in the above expansion, it is easy to show [29] that the coefficients a_{ij}'s are related to various electron-electron interactions. The atomic orbital

eigen value ϵ_i of the level i is related [30] to the total energy as

$$\epsilon_i = \frac{\partial E}{\partial n_i} = 2[\sum_j a_{ij} n_j] + b_i$$

Then the charge transfer energy, Δ, defined as

$$\Delta = E(...n_d + 1...n_p - 1...) - E(...n_d...n_p...)$$

is readily given by

$$\Delta = \epsilon_d - \epsilon_p + \frac{1}{2} U_{dd} \tag{1}$$

Thus, Δ and the difference in the orbital eigen values, $\epsilon_d - \epsilon_p$ are linearly related with the difference being half of the intraatomic Coulomb strength within the $3d$ electrons. In Fig. 8, we have plotted the values of Δ obtained from various high energy spectroscopic results as a function of the orbital energy difference, $\epsilon_d - \epsilon_p$, calculated in the present work. The straight line with a unity slope represents the expected dependence of Δ on $\epsilon_d - \epsilon_p$ in absence of Coulomb interaction. With the sole exception of the case of V, all experimental estimates of Δ is larger than that represented by the straight line; this clearly indicates the presence of finite Coulomb interaction strengths in all these cases. We however would not like to estimate U_{dd} from the difference between the experimentally estimated Δ values and the value (represented by the straight line in Fig. 8) expected in absence of U_{dd}, since the uncertainty in estimating Δ from experiment can be very large (as large as $\pm$ 2 eV). This is also possibly the reason why the Δ value in the case of the vanadium compound has been estimated lower than the straight line. The present results suggest that the estimate of $\epsilon_d - \epsilon_p$ in this work can be used to guide the choice for Δ via the equation 1. Essentially, equation 1 gives a relationship between Δ and U_{dd}, since $\epsilon_d - \epsilon_p$ is estimated here, this leaves only one parameter (U_{dd} or Δ) to be determined from experimental results.

On many occassions, it is desirable to know how $pd\sigma$ changes with the distance between the transition metal and the oxygen atom in a compound. This may be very useful in describing the electronic structure of any compound under pressure, or in the case of compounds,

such as $LaMnO_3$, where various transition metal-oxygen distances are observed. Thus, there have been many attempts to express the functional dependence between $pd\sigma$ and r_{M-O}. It was shown earlier that the interatomic matrix-elements are supposed to scale with distance as $1/r^{l+l'+1}$ [32], where l and l′ are the angular momenta of the orbitals involved. Thus, for $p-d$ interactions, the matrix elements scale as $1/r^4$. In order to obtain an *ab-initio* estimate of the functional dependence, we have calculated the band structure of $LaCoO_3$ with different lattice parameters. The different sets of band dispersions have been analysed in terms of the same tight-binding Hamiltonian with overlap included. The parameters in each case were obtained by the previously discussed least-squared error fitting procedure. We have plotted the $pd\sigma$ thus obtained as a function of r_{Co-O} for the eight different calculations in a $\log_{10}$-$\log_{10}$ plot. The smallest r_{Co-O} corresponds to a 4% contraction while the largest value corresponds to a 9.9% expansion over the equilibrium r_{Co-O}. Over this entire range, $\log_{10}(pd\sigma)$ is found to vary approximately linearly with $\log_{10}(r_{Co-O})$ with a slope of -3.04±0.02. This implies that $pd\sigma$ varies approximately as $1/r^3_{Co-O}$ which in other terms is $1/r^{l+l'}$ in contrast to the earlier expectation of $1/r^{l+l'+1}$ dependence.

In conclusion, the electronic structure of the $LaMO_3$ series have been studied by mapping the results of a tight-binding Hamiltonian with nearest-neighbor interactions onto the *ab-initio* band structure results for M=Ti-Ni. All the interaction parameters are found to exhibit systematic changes across the transition metal series. The estimates of various interaction strengths compare well with estimates obtained from spectroscopic data, wherever available. The hopping interaction strength, $pd\sigma$ is found to depend on the transition metal-oxygen separation, r approximately as r^{-3}.

Acknowledgment

D.D.S. thanks Dr. M. Methfessel, Dr. A. T. Paxton, and Dr. M. van Schiljgaarde for making the LMTO-ASA band structure program available and Dr. S. Krishnamurthy for initial help in setting up the LMTO-ASA program. N. S. and P. M. thank the Council of Scientific and Industrial Research, Government of India for Research Fellowships.

REFERENCES

* Also at the Jawaharlal Nehru Centre for Advanced Scientific Research, Bangalore.

[1] G. A. Sawatzky and J. W. Allen, Phys. Rev. Lett. **53**, 2239 (1984); J. Zannen, G. A. Sawatzky and J. W. Allen, Phys. Rev. Lett. **55**, 418 (1985).

[2] D. D. Sarma, H. R. Krishnamurthy, Seva Nimkar, S. Ramasesha, P. P. Mitra and T. V. Ramakrishnan, Pramana-J. Phys. **38**, L531 (1992); Seva Nimkar, D. D. Sarma, H. R. Krishnamurthy and S. Ramasesha, Phys. Rev. B **48**, 7355 (1993).

[3] A. Fujimori, A. E. Bocquet, K. Morikawa, K. Kobayashi, T. Saitoh, Y. Tokura, I. Hase and M. Onoda, J. Phys. Chem. Solids (in press); A. E. Bocquet, T. Mizokawa, K. Morikawa, A. Fujimori, S. R. Barman, K. Maiti, D. D. Sarma, Y. Tokura and M. Onoda, Phys. Rev. B **53**, 1161 (1996); T. Saitoh, A. E. Bocquet, T. Mizokawa, H. Namatame, A. Fujimori, M. Abbate, Y. Takeda and M. Takano, Phys. Rev. B **51**, 13942 (1995).

[4] G. van der Laan, C. Westra, C. Haas and G. A. Sawatzky, Phys. Rev. B **23**, 4369 (1981); J. Zaanen, C. Westra and G. A. Sawatzky, Phys. Rev. B **33**, 8060 (1986).

[5] A. Chainani, M. Mathew and D. D. Sarma, Phys. Rev. B **48**, 14818 (1993); A. Chainani, M.Mathew and D. D. Sarma, Phys. Rev. B **46**, 9976 (1992); S. R. Barman and D. D. Sarma, Phys. Rev. B **49**, 13979 (1994); A. Chainani, M. Mathew and D. D. Sarma, Phys. Rev. B **47**, 15397 (1993); S. R. Barman, A. Chainani and D. D. Sarma, Phys. Rev. B **49**, 8475 (1994).

[6] D. D. Sarma, Phys. Rev. B **37**, 7948 (1988); D. D. Sarma and S. G. Ovchinnikov, Phys. Rev. B **42**, 6817 (1990); D. D. Sarma and A. Chainani, J. Solid State Chem. **111**, 208 (1994).

[7] D. D. Sarma, J. Phys. Soc. Jpn. **65** (1996) (in press).

[8] D. D. Sarma, N. Shanthi, S. R. Barman, N. Hamada, H. Sawada and K. Terakura, Phys.

Rev. Lett. **75**, 1126 (1995); D. D. Sarma, N. Shanthi and Priya Mahadevan, Phys. Rev. B (MS# BL5911).

[9] R. von Helmolt, J. Wecker, B. Holzaphel, L. Schultz and K. Samwer, Phys. Rev. Lett. **71**, 2331 (1993); A. Asamitsu, Y. Moritomo, Y. Tomioka, T. Arima and Y. Tokura, Nature **373**, 407 (1995); Y. Okimoto, T. Katsufuji, T. Ishikawa, A. Urushibara, T. Arima and Y. Tokura, Phys. Rev. Lett. **75**, 109 (1995); Y. Tokura, Y. Taguchi, Y. Okada, Y. Fujishima, T. Arima, K. Kumagai and Y. Iye, Phys. Rev. Lett. **70**, 2126 (1993); F. Inaba, T. Arima, T. Ishikawa, T. Katsufuji and Y. Tokura, Phys. Rev. B **52**, 2221 (1995); X. Obradors, L. M. Paulius, M. B. Maple, J. B. Torrance, A. I. Nazzal, J. Fontcuberta and X. Granados, Phys. Rev. B **47**, 12353 (1993).

[10] L. F. Mattheiss, Phys. Rev. B **5**, 290 (1972).

[11] J. B. Grant and A. K. McMahan, Physica C **162-164**, 1439 (1989).

[12] L. F. Mattheiss, Phys. Rev. Lett. **58**, 1028 (1987).

[13] T. Oguchi, Phys. Rev. B **51**, 1385 (1995).

[14] O. Gunnarsson, O. K. Andersen, O. Jepsen and J. Zaanen, Phys. Rev. B **39**, 1708 (1989).

[15] David A. Maclean, Hok-Nam NG and J. E. Greeden, J. Solid State Chem. **30**, 35 (1979).

[16] P. Bordet, C. Chaillout, M. Marezio, Q. Huang, A. Santoro, S-W. Cheong, H. Takagi, C. S. Oglesby and B. Batlogg, J. Solid State Chem. **106**, 253 (1993).

[17] C. P. Khattak and D. E. Cox, J. Appl Cryst. **10**, 405 (1977);

[18] M. Marezio and P. D. Dernier, Mater. Res. Bull. **6**, 23 (1971);

[19] G. Thornton, B. C. Tofield and A. W. Hewat, J. Solid State Chem. **61**, 301 (1986);

[20] J. L. Garcia-Munoz, J. Rodriguez-Carvajal, P. Lacorre and J. B. Torrance, Phys. Rev.

B **46**, 4414 (1992).

[21] J. B. A. A. Elemans, B. van Larr, K. R. van der Veen, and B. O. Loopstra, J. Solid State Chem. **3**, 238 (1971);

[22] B. C. Tofield and W. R. Scott, J. Solid State Chem. **10**, 183 (1974).

[23] A. Fujimori, E. Takayama-Muromachi, Y. Uchida and B. Okai, Phys. Rev. B **35**, 8814 (1987).

[24] J. C. Slater and G. F. Koster, Phys. Rev. **94**, 1498 (1954).

[25] L. F. Mattheiss, Phys. Rev. B **2**, 3918 (1970).

[26] Warren E. Pickett and David J. Singh, Phys. Rev B**53**, 1146 (1996).

[27] S. Satpathy, Zoran S. Popović and Filip R. Vukajlović, Phys. Rev. Lett **76**, 960 (1996).

[28] Hideaki Sawada, Noriaki Hamada, Kiyoyuki Terakura and Toshio Asada, (to be published in May 15 issue of Phys Rev B).

[29] D. D. Sarma, Reviews of Solid State Sciences **5**, 401 (1991).

[30] J. C. Slater and J. H. Wood, Int. J. Quantum Chem. **45**, 3 (1971); J. C. Slater, T. M. Wilson and J. H. Wood, Phys. Rev. **179**, 28 (1969).

[31] O. K. Anderson, Phys. Rev. B **12** 3060 (1975); O. K. Anderson and R. V. Kasowski, Phys. Rev. B **4** 1064 (1971); O. K. Anderson, Solid State Commun. **13**, 133 (1973).

[32] O. K. Andersen, W. Klose and H. Nohl, Phys. Rev. B **17**, 1209 (1978).

I. FIGURE CAPTIONS

Fig.1 The LMTO DOS for $LaMnO_3$ (solid line) alongwith the partial DOS for the Oxygen p states (dotted line) as well as for the Mn d states (dashed line).

Fig.2 (a). The LMTO band dispersions, and (b) the best-fit TB band dispersions for $LaMnO_3$ along the symmetry directions ΓL, LF, FZ, $Z\Gamma$.

Fig.3 The LMTO DOS for $LaFeO_3$ (solid line) alongwith the partial DOS for the Oxygen p states (dotted line) as well as for the Fe d states (dashed line).

Fig.4 (a). The LMTO band dispersions, and (b) the best-fit TB band dispersions for $LaFeO_3$ along the symmetry directions ΓX, ΓY, ΓZ and ΓR.

Fig.5 The variations of the interaction strengths $sd\sigma$, $pp\sigma$, $pp\pi$, $pd\sigma$ and $pd\pi$ across the transition metals series, Ti-Ni. The inset shows the interatomic distances between the metal-oxygen (r_{M-O}) and the oxygen-oxygen (r_{O-O}) sites in Åfor the series.

Fig.6 The variation of ϵ_p-ϵ_d across the transition metals series, Ti-Ni.

Fig.7 A comparison of the calculated $(pd\sigma)_{calc}$ to the values estimated from experiments, $(pd\sigma)_{expt}$ by different groups (Tokyo and Bangalore). The solid line has been drawn for $(pd\sigma)_{calc}$ equal to $(pd\sigma)_{expt}$ and the dashed lines indicate the trends seen in the data from different groups.

Fig.8 A comparison of the calculated value of $\epsilon_d - \epsilon_p$ with the experimentally obtained Δ. The solid line represents Δ=$\epsilon_d - \epsilon_p$.

Fig.9 The variation of $\log_{10}(pd\sigma)$ with $\log_{10}(r_{Co-O})$ in $LaCoO_3$.

TABLES

TABLE I. Estimates of tight-binding parameters by a least-squared-error fitting of LMTO results including orbital overlaps. The numbers in parentheses have been obtained by fitting only the transition metal d bands.

Compound	$sd\sigma$ (eV)	$pp\sigma$ (eV)	$pp\pi$ (eV)	$pd\sigma$ (eV)	$pd\pi$ (eV)	$\epsilon_d - \epsilon_p$ (eV)
$LaTiO_3$	-2.54	0.58	-0.17	-2.33	1.42	6.01
$LaVO_3$	-2.62	0.73	-0.14	-2.30	1.27	4.80
	(-2.59)	(0.73)	(-0.14)	(-2.32)	(1.28)	(4.80)
$LaCrO_3$	-2.44	0.72	-0.16	-2.25	1.19	3.86
	(-2.47)	(0.72)	(-0.16)	(-2.25)	(1.19)	(3.86)
$LaMnO_3$	-2.21	0.70	-0.16	-1.99	1.10	3.12
	(-2.22)	(0.70)	(-0.16)	(-1.99)	(1.10)	(3.12)
$LaFeO_3$	-1.73	0.64	-0.15	-1.66	0.86	1.98
	(-1.74)	(0.64)	(-0.15)	(-1.66)	(0.86)	(1.98)
$LaCoO_3$	-1.95	0.77	-0.24	-1.72	1.02	1.63
	(-1.96)	(0.77)	(0.24)	(-1.72)	(1.02)	(1.63)
$LaNiO_3$	-1.59	0.76	-0.14	-1.57	0.97	0.69
	(-1.60)	(0.76)	(-0.14)	(-1.55)	(0.95)	(0.75)

TABLE II. Estimates of tight-binding parameters by least-squared-error fitting of LMTO results with the assumption of orthonormal basis functions. The numbers in parentheses have been obtained by fitting only the transition metal d bands.

Compound	$sd\sigma$ (eV)	$pp\sigma$ (eV)	$pp\pi$ (eV)	$pd\sigma$ (eV)	$pd\pi$ (eV)	$\epsilon_d - \epsilon_p$ (eV)
$LaTiO_3$	-2.89	0.52	-0.11	-2.50	1.49	5.91
$LaVO_3$	-2.69	0.47	-0.07	-2.44	1.23	4.70
	(-2.71)	(0.47)	(-0.07)	(-2.45)	(1.27)	(4.66)
$LaCrO_3$	-2.34	0.50	-0.08	-2.37	1.15	3.79
	(-2.36)	(0.50)	(-0.08)	(-2.38)	(1.18)	(3.76)
$LaMnO_3$	-2.09	0.57	-0.10	-2.11	0.97	3.10
	(-2.13)	(0.57)	(-0.10)	(-2.17)	(1.08)	(2.93)
$LaFeO_3$	-1.68	0.50	-0.08	-1.72	0.82	1.85
	(-1.67)	(0.50)	(-0.08)	(-1.72)	(0.83)	(1.85)
$LaCoO_3$	-1.69	0.62	-0.12	-1.91	0.89	1.50
	(-1.72)	(0.62)	(-0.12)	(-1.92)	(0.92)	(1.44)
$LaNiO_3$	-1.40	0.66	-0.12	-1.67	0.77	0.69
	(-1.62)	(0.66)	(-0.12)	(-1.73)	(0.88)	(0.4)

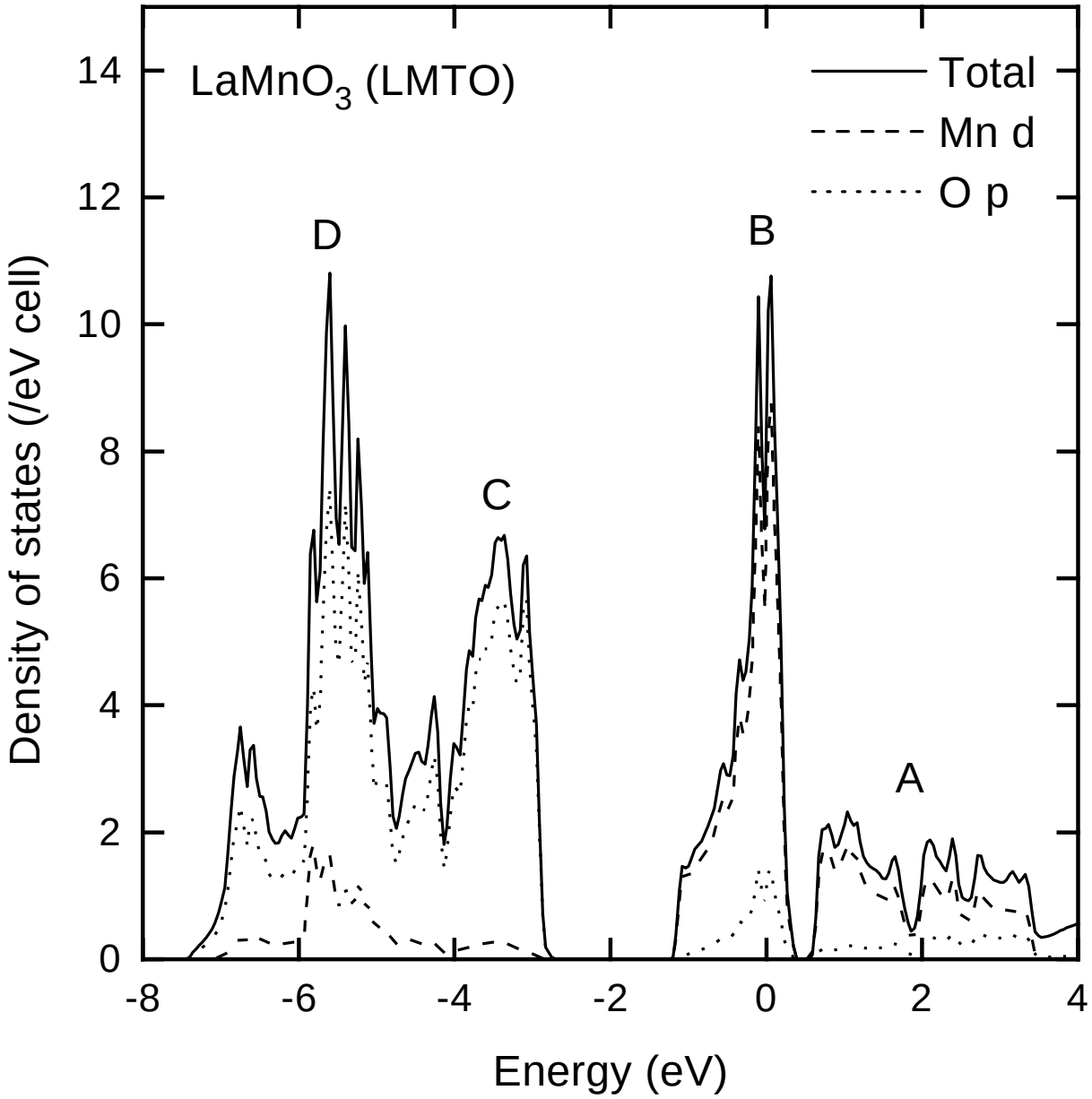

Fig.1
Priya Mahadevan,
N. Shanthi and
D. D. Sarma

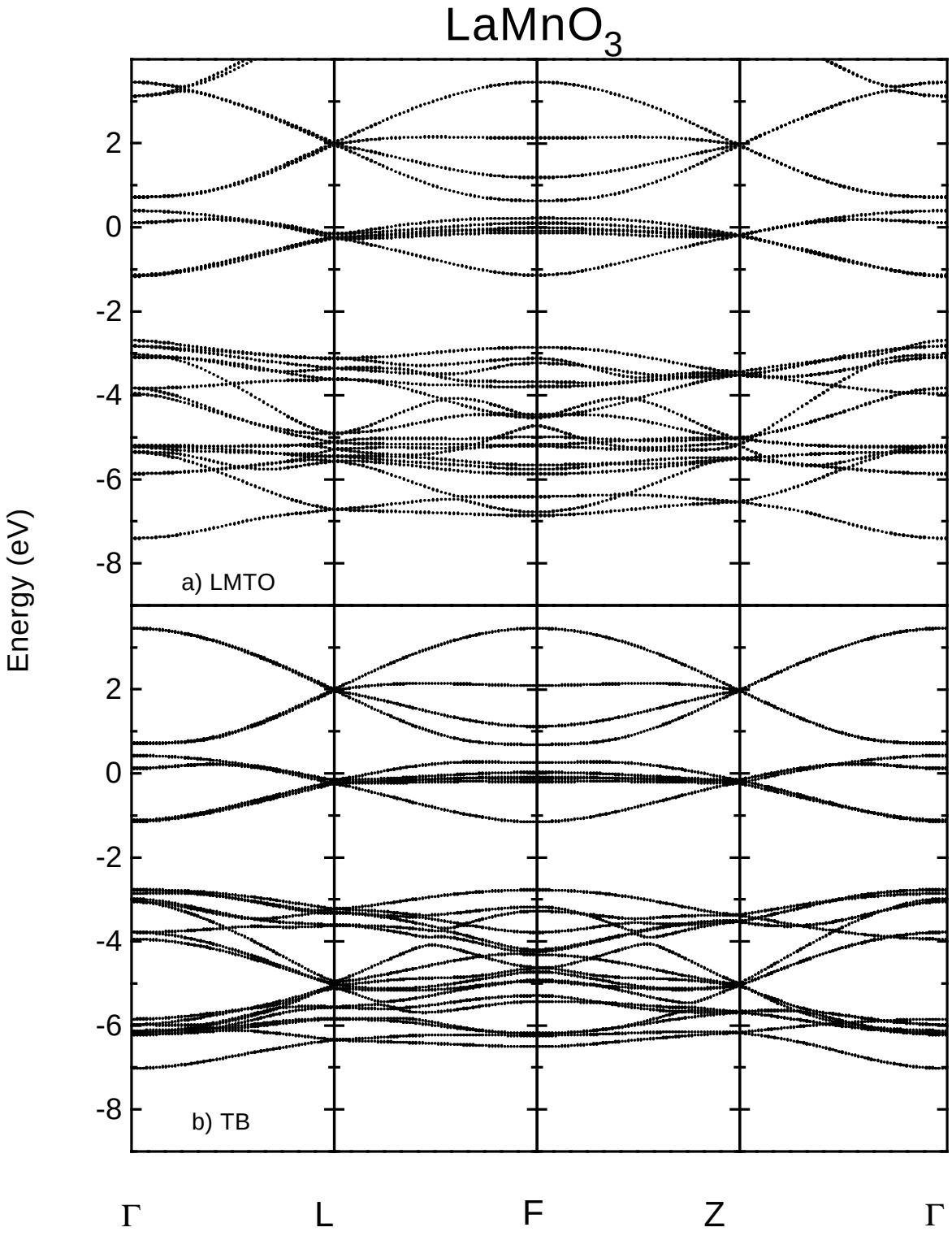

Fig. 2
Priya Mahadevan,
N. Shanthi and
D. D. Sarma

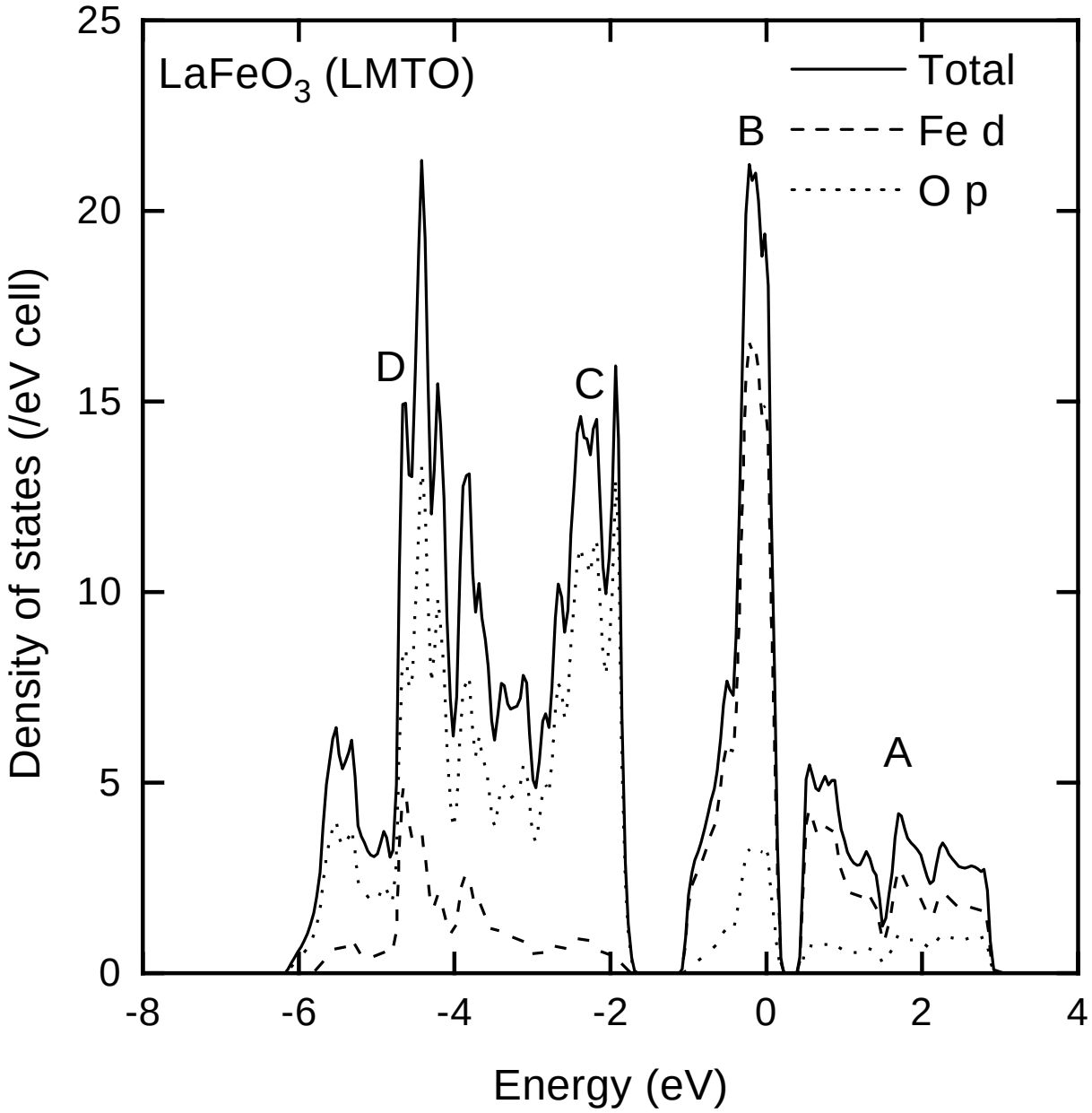

Fig. 3
Priya Mahadevan,
N. Shanthi and
D. D. Sarma

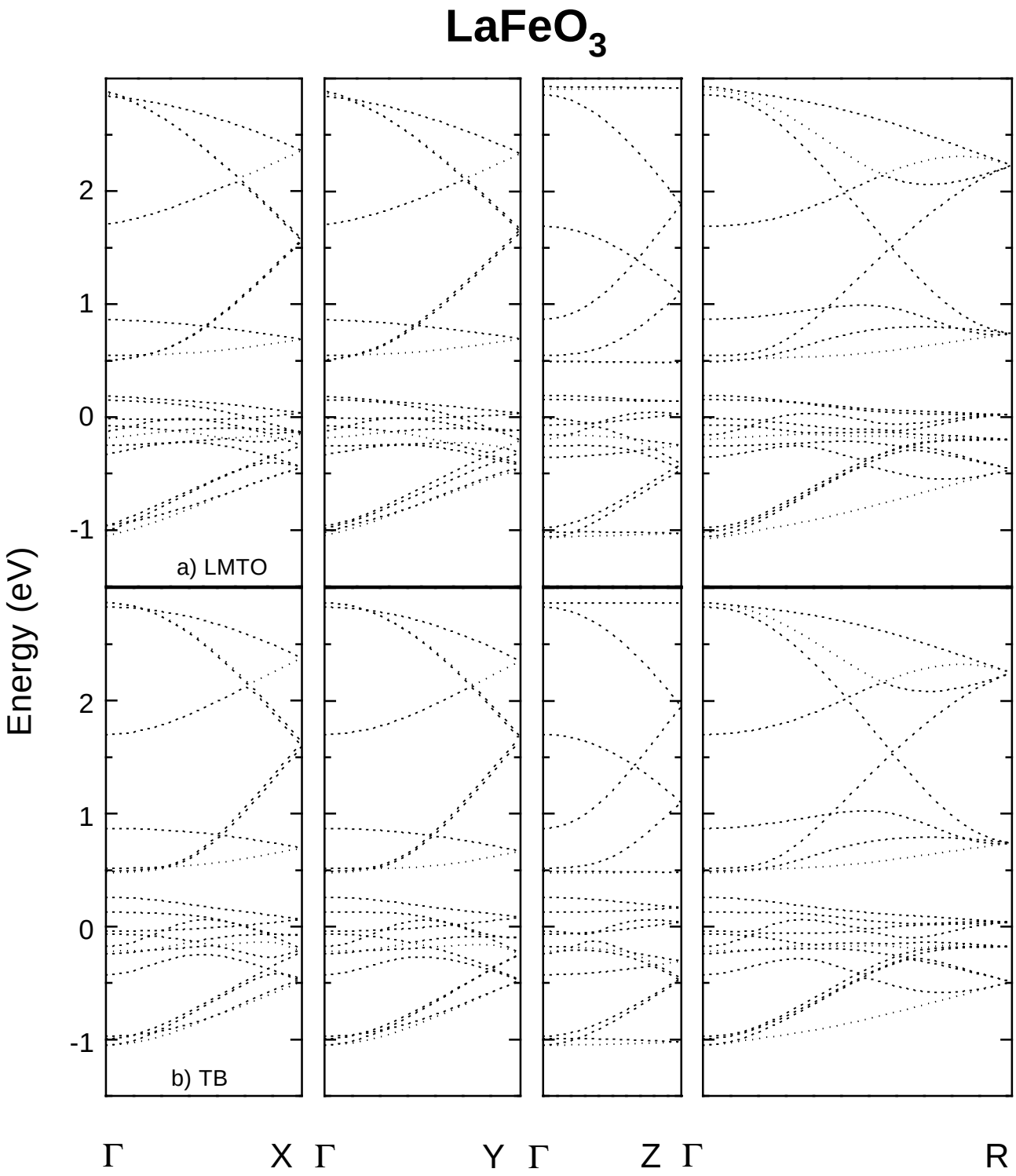

Fig. 4
Priya Mahadevan,
N. Shanthi and
D. D. Sarma

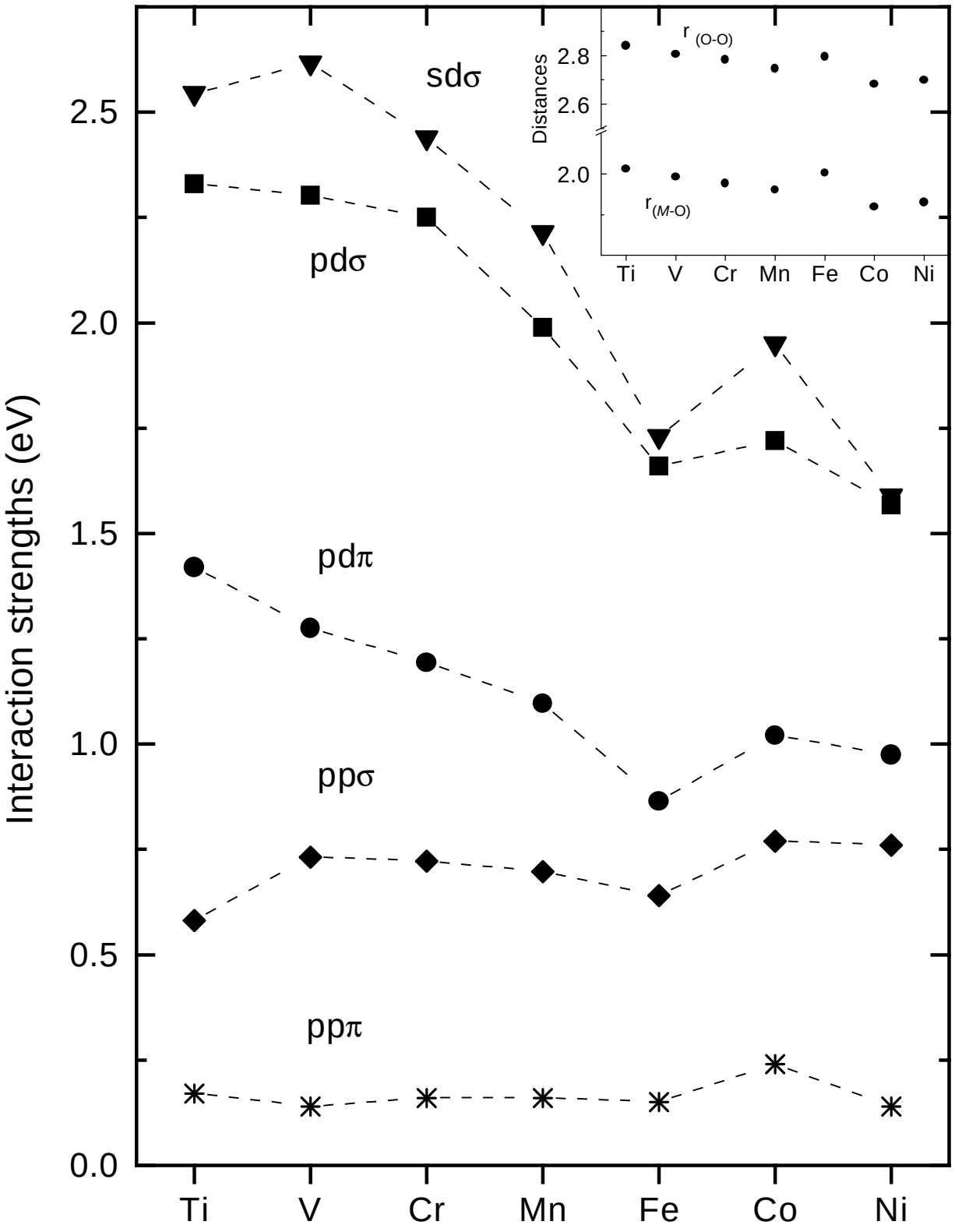

Fig. 5
Priya Mahadevan,
N. Shanthi and
D. D. Sarma

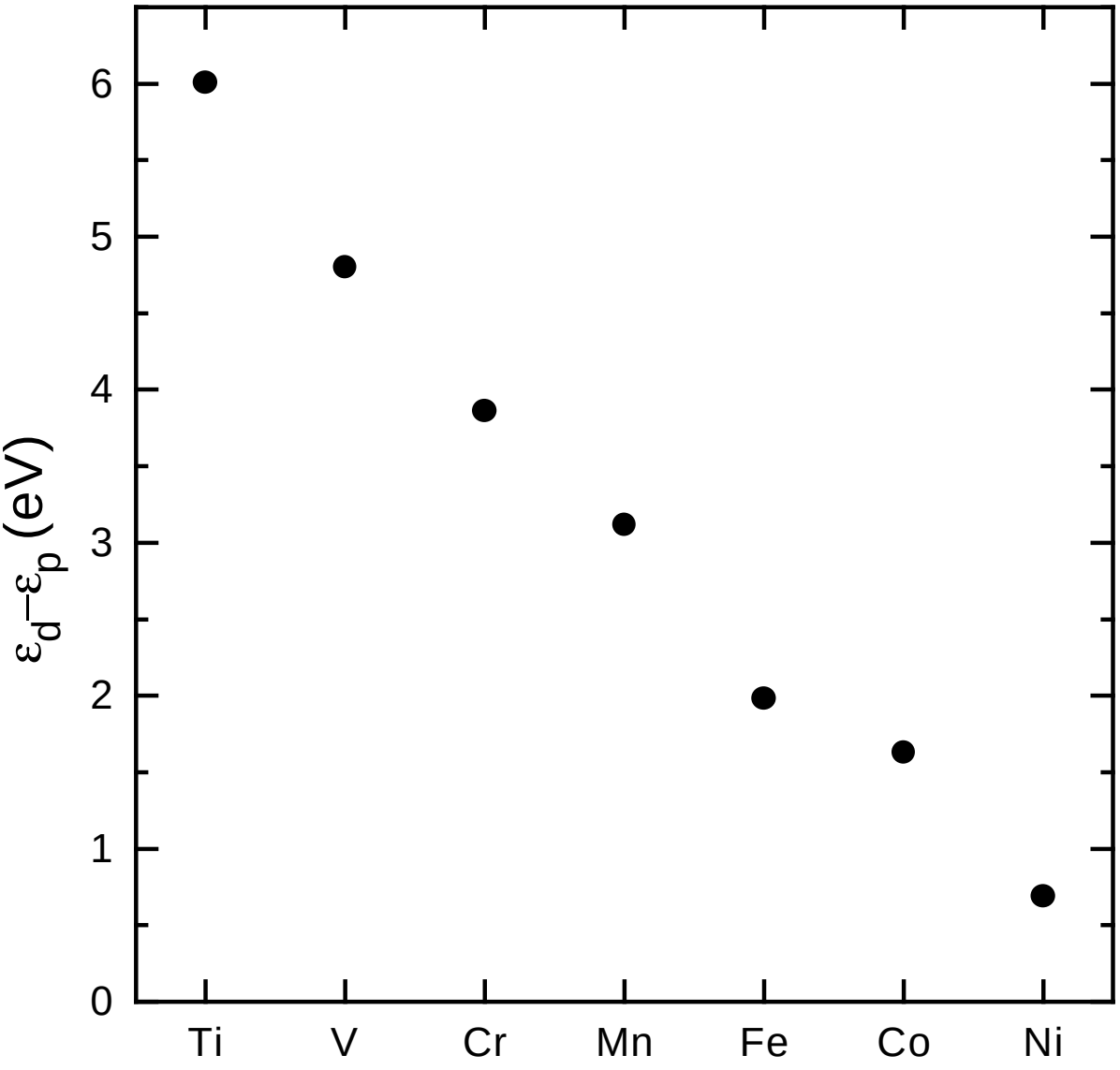

Fig. 6
Priya Mahadevan,
N. Shanthi and
D. D. Sarma

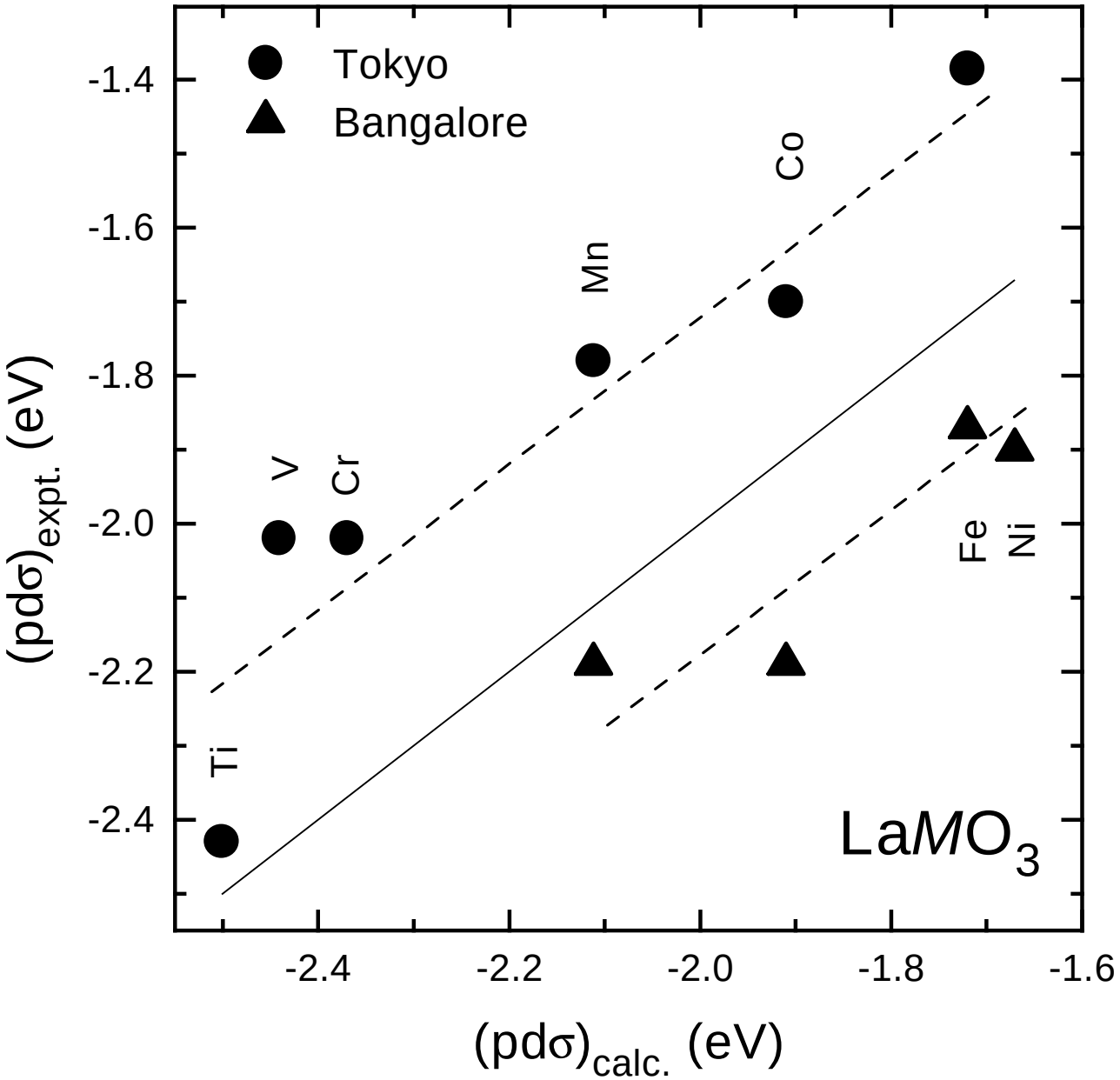

Fig. 7
Priya Mahadevan,
N. Shanthi and
D.D. Sarma

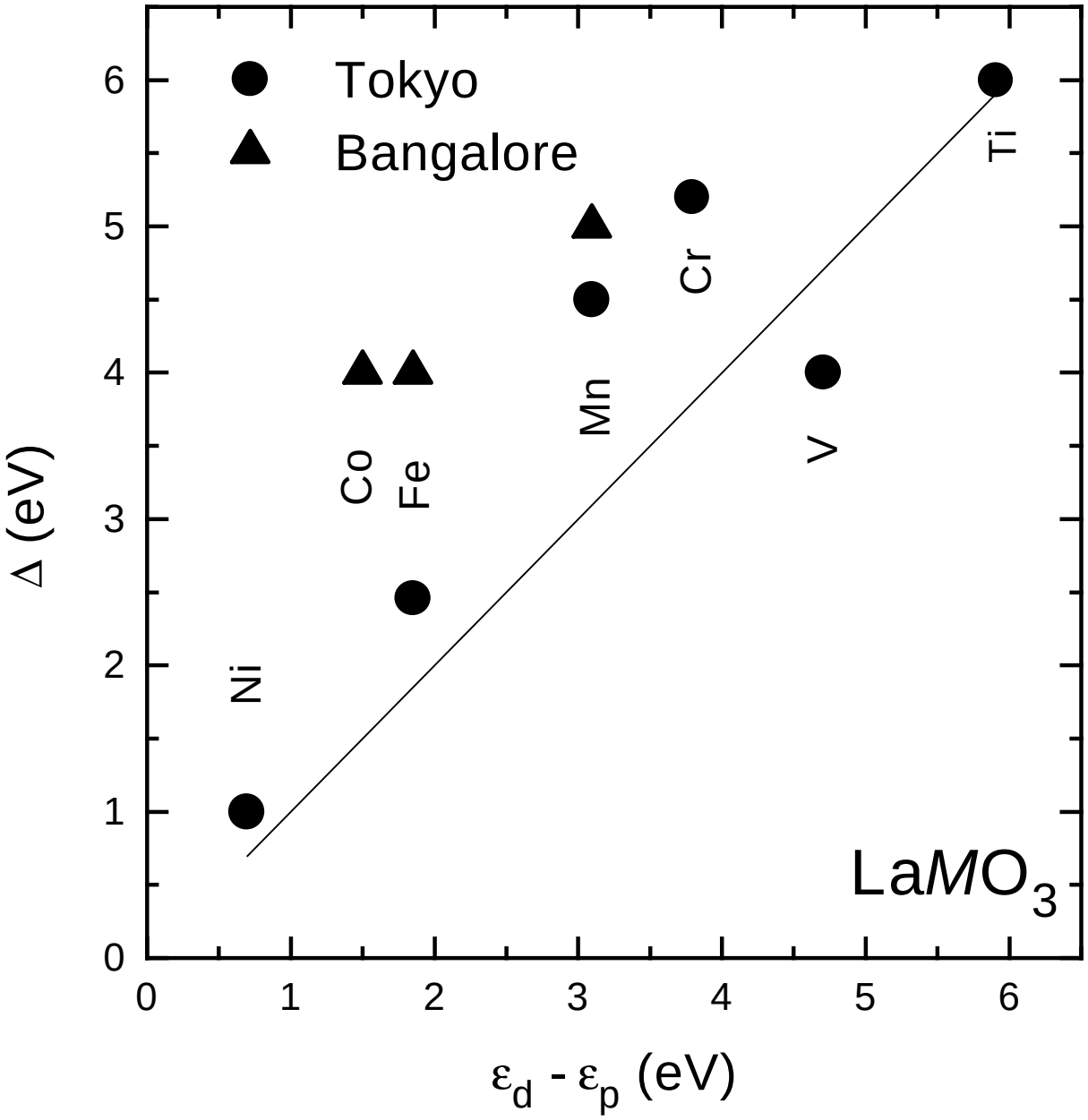

Fig. 8
Priya Mahadevan,
N. Shanthi and
D. D. Sarma

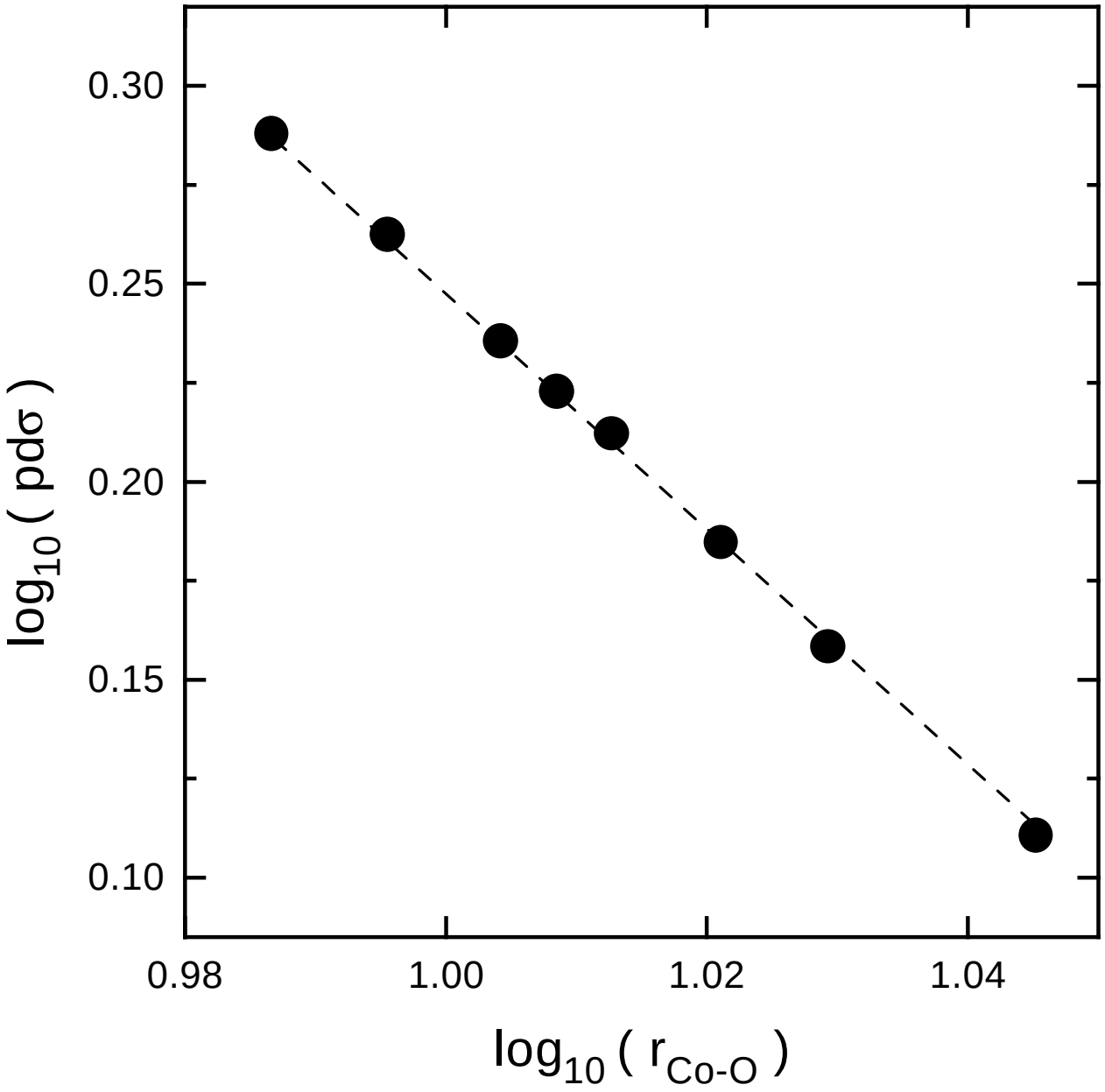

Fig. 9
Priya Mahadevan,
N. Shanthi and
D. D. Sarma